Osteoarthritis and Cartilage 27 (2019) 965–976

Osteoarthritis and Cartilage

Pharmacological inhibition of mTORC1 but not mTORC2 protects against human disc cellular apoptosis, senescence, and extracellular matrix catabolism through Akt and autophagy induction

Y. Kakiuchi † [a], T. Yurube † * [a], K. Kakutani † [a], T. Takada ‡ [b], M. Ito † [a], Y. Takeoka † [a], Y. Kanda † [a], S. Miyazaki † [a], R. Kuroda † [a], K. Nishida † [a]

† *Department of Orthopaedic Surgery, Kobe University Graduate School of Medicine, 7-5-1 Kusunoki-cho, Chuo-ku, Kobe 650-0017, Japan*
‡ *Department of Orthopaedic Surgery, Kenshinkai Kobe Hokuto Hospital, 37-3 Yamada-cho Shimotanigami Aza Umekidani, Kita-ku, Kobe 651-1243, Japan*

ARTICLE INFO

Article history:
Received 21 July 2018
Accepted 25 January 2019

Keywords:
Intervertebral disc
Nucleus pulposus cells
Mammalian target of rapamycin (mTOR)
Akt
Autophagy
Spine

SUMMARY

Objective: The mammalian target of rapamycin (mTOR) is a serine/threonine kinase that integrates nutrients to execute cell growth. We hypothesized that mTOR is influential in the intervertebral disc—largest avascular, low-nutrient organ. Our objective was to identify the optimal mTOR inhibitor for treating human degenerative disc disease.

Design: mTOR complex 1 (mTORC1) regulates p70/ribosomal S6 kinase (p70/S6K), negatively regulates autophagy, and is controlled by Akt. Akt is controlled by phosphatidylinositol 3-kinase (PI3K) and mTOR complex 2 (mTORC2). mTORC1 inhibitors—rapamycin, temsirolimus, everolimus, and curcumin, mTORC1&mTORC2 inhibitor—INK-128, PI3K&mTOR inhibitor—NVP-BEZ235, and Akt inhibitor—MK-2206—were applied to human disc nucleus pulposus (NP) cells. mTOR signaling, autophagy, apoptosis, senescence, and matrix metabolism were evaluated.

Results: mTORC1 inhibitors decreased p70/S6K but increased Akt phosphorylation, promoted autophagy with light chain 3 (LC3)-II increases and p62/sequestosome 1 (p62/SQSTM1) decreases, and suppressed pro-inflammatory interleukin-1 beta (IL-1β)-induced apoptotic terminal deoxynucleotidyl transferase dUTP nick end labeling (TUNEL) positivity (versus rapamycin, 95% confidence interval (CI) −0.431 to −0.194; temsirolimus, 95% CI −0.529 to −0.292; everolimus, 95% CI −0.477 to −0.241; curcumin, 95% CI −0.248 to −0.011) and poly (ADP-ribose) polymerase (PARP) and caspase-9 cleavage, senescent senescence-associated beta-galactosidase (SA-β-gal) positivity (versus rapamycin, 95% CI −0.437 to −0.230; temsirolimus, 95% CI −0.534 to −0.327; everolimus, 95% CI −0.485 to −0.278; curcumin, 95% CI −0.210 to −0.003) and p16/INK4A expression, and catabolic matrix metalloproteinase (MMP) release and activation. Meanwhile, dual mTOR inhibitors decreased p70/S6K and Akt phosphorylation without enhanced autophagy and suppressed apoptosis, senescence, and matrix catabolism. MK-2206 counteracted protective effects of temsirolimus. Additional disc-tissue analysis found relevance of mTOR signaling to degeneration grades.

Conclusion: mTORC1 inhibitors—notably temsirolimus with an improved water solubility—but not dual mTOR inhibitors protect against inflammation-induced apoptosis, senescence, and matrix catabolism in human disc cells, which depends on Akt and autophagy induction.

* Address correspondence and reprint requests to: T. Yurube, MD, PhD, Department of Orthopaedic Surgery, Kobe University Graduate School of Medicine, 7-5-1 Kusunoki-cho, Chuo-ku, Kobe 650-0017, Japan. Tel: 81-78-382-5985; Fax: 81-78-351-6944.

E-mail addresses: yuji_uz_7@yahoo.co.jp (Y. Kakiuchi), takayuru-0215@umin.ac.jp (T. Yurube), kakutani@med.kobe-u.ac.jp (K. Kakutani), takada-t@hokuto-hp.or.jp (T. Takada), maito28710@yahoo.co.jp (M. Ito), yoshiki_tkk@hotmail.com (Y. Takeoka), youthfuldays_y_k@yahoo.co.jp (Y. Kanda), mghff229@yahoo.co.jp (S. Miyazaki), kurodar@med.kobe-u.ac.jp (R. Kuroda), kotaro@med.kobe-u.ac.jp (K. Nishida).

[a] Tel: 81-78-382-5985; Fax: 81-78-351-6944.
[b] Tel: 81-78-583-1771; Fax: 81-78-583-1784.

https://doi.org/10.1016/j.joca.2019.01.009

Introduction

Low back pain affects ~85% of people during their lives, decreases the workforce because of disability, and then increases medical expenses[1]. Annual health care costs of low back pain were estimated up to $102.0 billion in the US[2]. Low back pain is multifactorial; however, intervertebral disc degeneration is recognized as one of the independent causes[3].

The intervertebral disc has a complex structure with the nucleus pulposus (NP) encapsulated by the annulus fibrosus and endplates, resulting in the largest avascular organ in the body[4]. The nutritional supply to disc NP cells depends on diffusion through the endplates primarily, which is easily reduced by endplate calcification and subchondral bone sclerosis occurring with injury, smoking and/or aging[5]. Therefore, additional nutrient deprivation is a suspected contributor to disc degeneration[5].

Intervertebral disc degeneration is biochemically characterized by extracellular matrix degradation[4,6]. Matrix metabolism is regulated by the balance between catabolic enzymes, e.g., matrix metalloproteinases (MMPs), and their anti-catabolic molecules, e.g., tissue inhibitors of metalloproteinases (TIMPs)[7]. Increased MMPs relative to TIMPs are often observed in human clinical[8,9] and rodent experimental disc degeneration[10–12], leading to degradation of matrix components e.g., proteoglycans, principally aggrecan, and collagens predominantly type 2 in the NP[6].

Another major characteristic of disc degeneration is cell decrease, which primarily results from programmed cell death—apoptosis[13]. A notably high incidence of apoptosis is observed in human[14] and rodent disc aging and degeneration[12,15]. The incidence of irreversible cell growth arrest by aging—senescence[16]—also increases with human disc degeneration[17]. Furthermore, autophagy, the process by which cells break down and recycle their own damaged components[18], has gained increasing attention in the disc[19]. Autophagy is an important cell survival mechanism to sustain metabolism and to prevent the accumulation of damaged toxic proteins and organelles under stress, primarily nutrient deprivation[18]. In molecular signaling, autophagy is under the tight negative regulation by the mammalian target of rapamycin (mTOR)[20]. On the basis of the harsh disc environment: low nutrition, pH, and oxygen concentration, we hypothesized that resident cells would utilize autophagy and mTOR signaling to cope with these stressful conditions.

The mTOR is a serine/threonine kinase which integrates nutrients to execute cell growth and division[20]. The mTOR exists in two complexes of mTOR complex 1 (mTORC1) and mTOR complex 2 (mTORC2)[20]. Down-stream mTORC1 effectors including p70/ribosomal S6 kinase (p70/S6K) regulates cell proliferation, messenger RNA (mRNA) translation, and protein synthesis[20]. Then, mTORC1 is regulated by up-stream Akt, an essential pro-survival mediator by suppressing apoptosis[21]. Moreover, Akt phosphorylation is known as a major role of the class I phosphatidylinositol 3-kinase (PI3K) and mTORC2 [Fig. 1][20,21].

The mTOR is the central signal integrator for nutrients and energy, playing critical roles in cell growth and division[20]. Complete inhibition of mTOR would be harmful. In fact, homogenous mTOR deletion results in embryonic lethality[22]. Therefore, it is required to identify which subunit(s) of mTOR exerts beneficial effects. Although we previously reported effects of mTOR-signaling modulation by the RNA interference technique in human disc cells[23], in clinical use, pharmacological modulation is favorable compared to gene-silencing therapy because of the safety issue. Rapamycin, an initially isolated mTORC1 inhibitor, extends mammalian lifespan[24] and also plays protective roles in human chondrocytes[25]. Despite striking effectiveness of rapamycin[24,25], rapamycin is not widely used clinically because of its poor water solubility, resulting in only

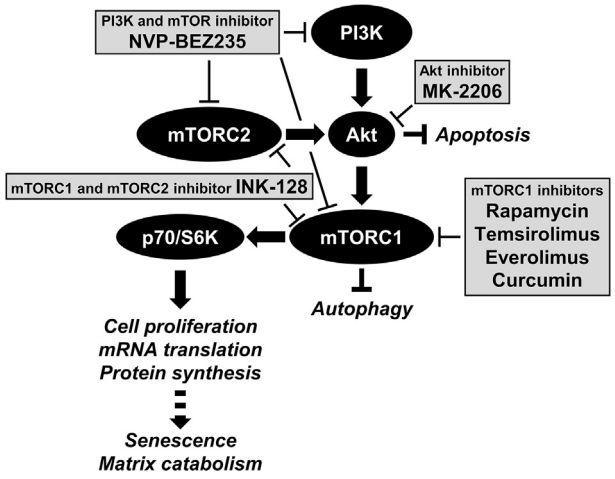

Fig. 1. Schematic illustration of the mTOR-signaling pathway. The mTOR is a serine/threonine kinase that integrates nutrients to execute cell growth and division. The mTOR exists in two complexes of mTORC1 and mTORC2. Down-stream effectors of mTORC1 including p70/S6K regulate cell proliferation, mRNA translation, and protein synthesis. Autophagy is under the tight negative regulation of mTORC1. The mTORC1 is regulated by the up-stream class I PI3K followed by Akt, an essential pro-survival mediator by suppressing apoptosis. Senescence and matrix catabolism are also affected by mTOR signaling. To analyze cascade-dependent roles of mTOR signaling, mTORC1 inhibitors—rapamycin, temsirolimus, everolimus, and curcumin, a dual mTORC1 and mTORCC2 inhibitor—INK-128, a dual PI3K and mTOR inhibitor—NVP-BEZ235, and/or an allosteric Akt inhibitor—MK-2206—were applied.

oral administration, and serious adverse effects including immunosuppression[26]. Subsequently, derivatives of rapamycin—everolimus and temsirolimus—have been developed[27]. Everolimus is the second novel analog available orally. Temsirolimus is a pro-drug which can be given intravenously as well as orally. Including rapamycin, these agents are the first generation mTOR inhibitors. A natural polyphenol from the rhizomes of turmeric—curcumin—is also reported to inhibit mTOR signaling in various cancer cells[28]. Therefore, an *in vitro* study was designed to identify the most suitable mTORC1 inhibitor for treating human degenerative disc disease. No comparative studies of mTORC1 inhibitors have been reported in disc cells or chondrocytes. Then, our previous study found that disc cells increased Akt phosphorylation by mTORC1 suppression but decreased Akt phosphorylation by mTORC2 suppression[23]. Recently, the second generation mTOR inhibitors that block both of mTORC1 and mTORC2 have been developed[27]. Therefore, an additional *in vitro* study was designed to assess effects of dual mTOR inhibitors on human disc cells. In this study, a dual mTORC1 and mTORC2 inhibitor—INK-128[27], a dual PI3K and mTOR inhibitor—NVP-BEZ235[27], and an allosteric Akt inhibitor—MK-2206[29]—were tested. No mechanistic studies of dual mTOR inhibitors have been conducted in human disc cells or chondrocytes. Furthermore in the present study, *in vivo* involvement of mTOR signaling was explored in human degenerative disc tissues. No reports regarding autophagy levels based on disc degeneration grade have been published as well.

Materials and methods

Ethics statement

All experimental procedures were performed under the approval and guidance of the Institutional Review Board (160004) at Kobe University Graduate School of Medicine. Written informed consent was obtained from each patient in accordance with the principles of the Declaration of Helsinki and the laws and regulations of Japan.

Antibodies and reagents

The antibodies and reagents used are listed in Supplemental Table 1.

Cells

Human disc NP cells were isolated from patient specimens undertaking lumbar spine surgery for degenerative disease ($n = 28$: age, 65.0 ± 13.8 [27–83] years; male 12, female 16; Pfirrmann degeneration grade[30], 3.4± 0.5 [3–4]). Immediately after surgery, human disc NP tissues were collected from discarded surgical waste and digested in 1% penicillin/streptomycin-supplemented Dulbecco's modified Eagle's medium (DMEM) with 10% fetal bovine serum (FBS) and 0.114% collagenase type 2 for 1 h at 37°C. Isolated cells were grown to ~80% confluence as a monolayer in 1% penicillin/streptomycin-supplemented DMEM with 10% FBS at 37°C under 2% O_2 to simulate the physiologically hypoxic disc environment[5]. To retain the phenotype, only first-passage cells were used for evaluation.

Cells were pre-cultured in DMEM with 10% FBS for 60 h, followed by with 1% FBS 12 h, and then treated for 24 h. As drug treatment, mTORC1-inhibiting rapamycin, temsirolimus, everolimus, and curcumin, mTORC1-inhibiting and mTORC2-inhibiting INK-128, PI3K-inhibiting and mTOR-inhibiting NVP-BEZ235, and/or Akt-inhibiting MK-2206 were applied. The dimethyl sulfoxide was used as the vehicle of these agents (1:1000 dilution) because of their limited water solubility. Vehicle control was prepared for all experiments.

First, cell viability was assessed using the Cell Counting Kit-8 (CCK-8). Western blotting (WB) for mTOR signaling and autophagy was performed in cell protein extracts. Second, to simulate clinically relevant disease conditions[31], cells were also treated by interleukin-1 beta (IL-1β) at 10 ng/ml with media change to serum-free DMEM to analyze released proteins[23]. The IL-1β is a pro-inflammatory cytokine closely linked to the pathogenesis and severity of disc degeneration[31]. WB for apoptosis and senescence in cell protein extracts and matrix catabolism in supernatant protein extracts was conducted. Cells were also applied to terminal deoxynucleotidyl transferase dUTP nick end labeling (TUNEL) staining, senescence-associated beta-galactosidase (SA-β-gal) staining, and real-time reverse transcription–polymerase chain reaction (RT–PCR) for matrix components.

Cells of 1.5×10^5/well (6-well plate) for protein extraction and RNA isolation, 1.2×10^4/well (8-well chamber) for staining, and 5.0×10^3/well (96-well plate) for viability assay were distributed randomly. In each experiment, six cell samples from six patients were used throughout the tested drugs ($n = 6$). Cell samples collected abundantly were used across experiments. Consequently, total 28 patient samples were used *in vitro*. To reduce possible variations based on degeneration grade, only grade-3 and grade-4 disc cells were applied [Fig. 2].

Tissues

Portions of human disc NP tissues surgically obtained from the lumbar spine were carefully dissected and directly used for protein extraction ($n = 12$: age, 45.9 ± 21.0 [19–81] years; male 5, female 7; Pfirrmann degeneration grade, 3.3 ± 1.1 [2–5]) [Fig. 2].

Cell viability assay

Cell viability was assessed by CCK-8 dehydrogenase activity, the absorbance of which (450 nm) was measured using the Model 680 microplate reader.

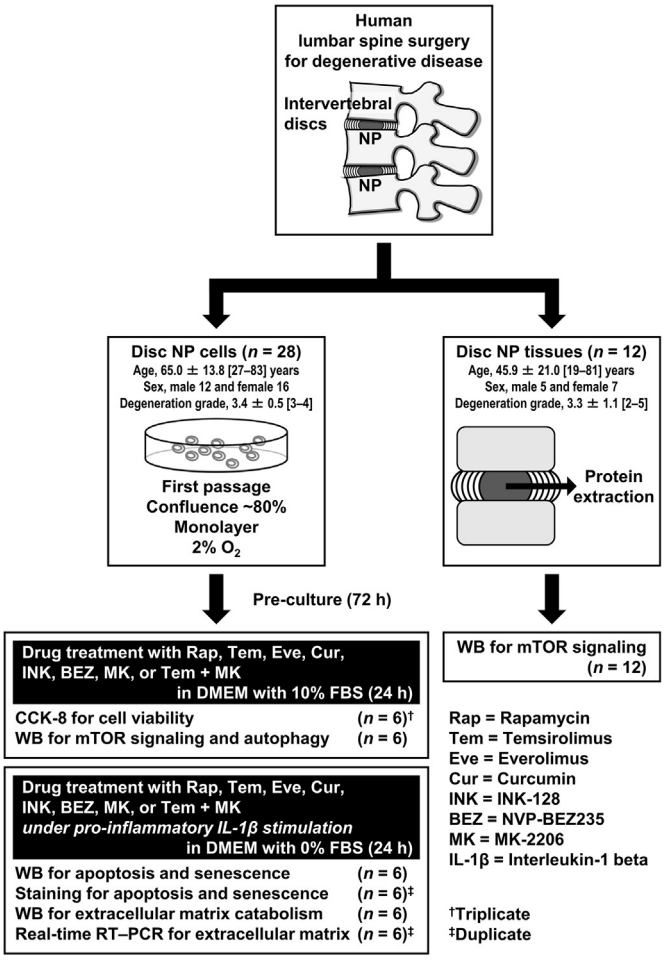

Fig. 2. Schematic illustration of the study design and sample number. Human lumbar spine surgery was performed in patients with degenerative disc disease. Immediately after surgery, human disc NP tissues were digested for cell isolation (total $n = 28$). Cells were grown to ~80% confluence as a monolayer in DMEM with 10% FBS at 37°C under 2% O_2. Only first-passage cells were pre-cultured in DMEM with 10% FBS for 60 h, followed by with 1% for FBS 12 h, and then treated for 24 h. As drug treatment, mTORC1-inhibiting rapamycin, temsirolimus, everolimus, and curcumin, mTORC1-inhibiting and mTORC2-inhibiting INK-128, PI3K-inhibiting and mTOR-inhibiting NVP-BEZ235, and/or Akt-inhibiting MK-2206 were applied. The vehicle control was prepared. First, CCK-8 assay for viability and WB for mTOR signaling and autophagy were performed in cells in DMEM with 10% FBS and drug supplementation. Second, under pro-inflammatory IL-1β stimulation, WB and staining assays for apoptosis and senescence and WB and real-time RT–PCR for extracellular matrix were performed in cells in DMEM with 0% FBS and drug supplementation. Each patient sample analysis was performed in duplicate in cell viability assay or triplicate in staining assays and real-time RT–PCR. The single data value was obtained by averaging technical replicates. These experiments were then conducted six times using six different patient samples ($n = 6$). Also, WB was conducted six times using six different patient samples and representative immunoblots of six similar results were shown ($n = 6$). In addition, portions of human disc NP tissues were directly used for protein extraction to assess mTOR signaling by WB (total $n = 12$).

Protein extraction

Cells were scraped off on ice in the 3-(*N*-morpholino)propanesulfonic acid buffer containing protease and phosphatase inhibitors. Soluble proteins were collected after centrifugation at 20,000 g for 15 min at 4°C. Non-serum-containing culture media were also collected, centrifuged at 1000 g for 10 min at 4°C to remove cellular debris, and concentrated using Amicon Ultra spin columns.

Tissues were homogenized using the MS-100R bead-beating disrupter for 30 s twice at 4°C in the T-PER tissue protein extraction

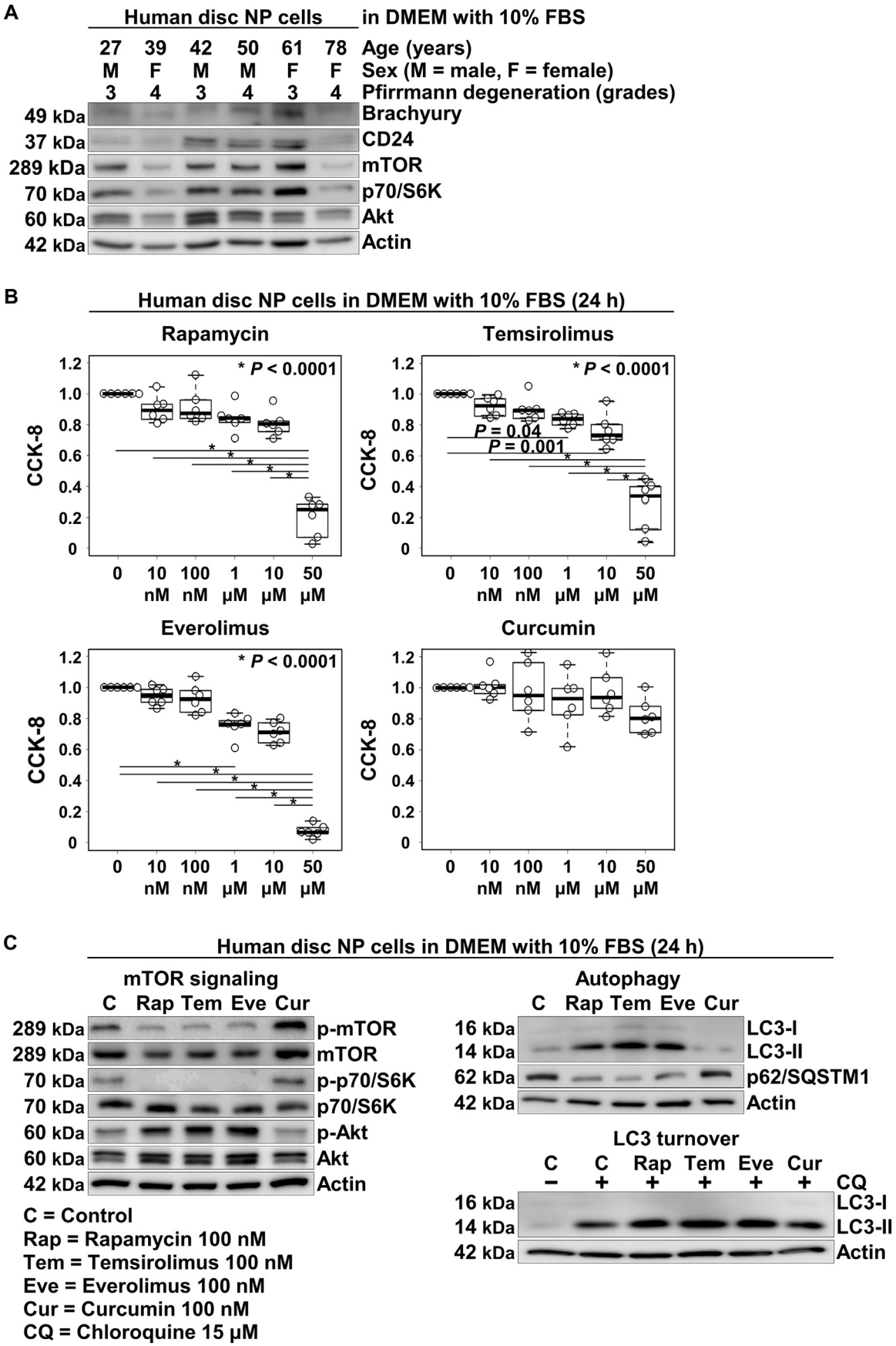
A
Human disc NP cells in DMEM with 10% FBS
27 39 42 50 61 78 Age (years)
M F M M F F Sex (M = male, F = female)
3 4 3 4 3 4 Pfirrmann degeneration (grades)
49 kDa Brachyury
37 kDa CD24
289 kDa mTOR
70 kDa p70/S6K
60 kDa Akt
42 kDa Actin
B
Human disc NP cells in DMEM with 10% FBS (24 h)
Rapamycin
Temsirolimus
Everolimus
Curcumin
CCK-8
* P < 0.0001
P = 0.04
P = 0.001
0 10 nM 100 nM 1 µM 10 µM 50 µM
C
Human disc NP cells in DMEM with 10% FBS (24 h)
mTOR signaling
C Rap Tem Eve Cur
289 kDa p-mTOR
289 kDa mTOR
70 kDa p-p70/S6K
70 kDa p70/S6K
60 kDa p-Akt
60 kDa Akt
42 kDa Actin
Autophagy
C Rap Tem Eve Cur
16 kDa LC3-I
14 kDa LC3-II
62 kDa p62/SQSTM1
42 kDa Actin
LC3 turnover
C C Rap Tem Eve Cur
– + + + + + CQ
16 kDa LC3-I
14 kDa LC3-II
42 kDa Actin
C = Control
Rap = Rapamycin 100 nM
Tem = Temsirolimus 100 nM
Eve = Everolimus 100 nM
Cur = Curcumin 100 nM
CQ = Chloroquine 15 µM

reagent with protease and phosphatase inhibitors. Soluble proteins were collected after centrifugation at 20,000 g for 15 min at 4°C.

Protein concentration was determined by the bicinchoninic acid assay. Samples were stored at −80°C.

Sodium dodecyl sulfate (SDS)–polyacrylamide gel electrophoresis and WB

Equal 30-μg amounts of protein were mixed with the electrophoresis sample buffer and boiled for 5 min before loading onto a 7.5–15.0% polyacrylamide gel. Separated proteins in the Tris–glycine–SDS buffer system were transblotted electrically and probed with primary antibodies for 12 h in 4°C (1:200–1:1000 dilution) followed by secondary antibodies (1:2000 dilution). Signals were visualized by enhanced chemiluminescence. Images were obtained using the Chemilumino analyzer LAS-3000 mini. Band intensity was quantified using the ImageJ software (http://rsweb.nih.gov/ij/).

WB was designed to analyze intracellular expression of disc NP-associated notochordal markers, brachyury and CD24[32], mTOR signaling-related mTOR, phosphorylated mTOR, Akt, phosphorylated Akt, p70/S6K, and phosphorylated p70/S6K[20], autophagy-related light chain 3 (LC3) and p62/sequestosome 1 (p62/SQSTM1)[33], apoptosis-related poly (ADP-ribose) polymerase (PARP)[34] and cleaved caspase-9[35], senescence-related p16/INK4A[36] in total cell or tissue protein extracts. Actin was used as a loading control. WB was also designed to analyze released expression of catabolic MMP-2, MMP-3, MMP-9, and MMP-13 and anti-catabolic TIMP-1 and TIMP-2 in supernatant protein extracts.

TUNEL staining

Apoptotic cells were identified using a fluorescein-labeled TUNEL assay kit[37]. Cells were fixed with 4% paraformaldehyde for 10 min. The 4′,6-diamidino-2-phenylindole (DAPI) was used for counterstaining. Images were photographed by the BZ-X700 microscope. The percentage of TUNEL-positive cells was calculated as relative to the number of DAPI-positive total cells, which were both counted in six random low-power fields (×100) using the ImageJ.

SA-β-gal staining

Cytochemical staining was performed to detect senescence using a SA-β-gal staining kit at pH 6[38]. The percentage of SA-β-gal-positive cells was similarly calculated in six random low-power fields (×100).

RNA isolation and real-time RT–PCR

Total RNA was extracted using the RNeasy mini kit, and 0.1 μg of RNA was reverse-transcribed with random primers. mRNA expression levels of anabolic *ACAN* encoding aggrecan and *COL2A1* encoding collagen type II alpha 1 chain relative to *glyceraldehyde 3-phosphate dehydrogenase* (*GAPDH*) were assessed by real-time RT–PCR using SYBR Green fluorescent dye. Good feasibility of *GAPDH* as an endogenous control for disc cells was established previously[39]. The primer sequences were as follows: *ACAN*, forward 5′-AAGAATCAAGTGGAGCCGTGTGTC-3′, reverse 5′-TGAGACCTTGTCCTGATAGGCACT-3′; *COL2A1*, forward 5′-AAGGTGCTTCTGGTCCTGCTG-3′, reverse 5′-GGGATTCCATTAGCACCATCTTTG-3′; *GAPDH*, forward 5′-GAGGCCGGTGCTGAGTAT-3′, reverse 5′-GCGGAGATGATGACCCTTTTGG-3′. The established primer sequences were found from prior reports[40] or purchased from Takara Bio. Measurements were performed using the ABI Prism 7500 real-time PCR system. Melting curve analysis was performed using the Dissociation Curves software to ensure that only a single product was amplified. Relative mRNA expression was analyzed using the $2^{-\Delta\Delta Ct}$ method[41]. The vehicle control value was set as 1.

Statistical analysis

In vitro, each patient sample analysis was performed in duplicate in cell viability assay or triplicate in staining assays and real-time RT–PCR (2 or 3 technical replicates). The single data value was obtained by averaging these replicates. These experiments were then conducted six times using six different patient samples (6 biological replicates) ($n = 6$). WB was also conducted six times using six different patient samples and representative immunoblots of six similar results were shown ($n = 6$). *In vivo*, WB was conducted using 12 different patient samples ($n = 12$).

In cell viability assay, dose-dependent effects of the agent were calculated as relative scores of the vehicle control. In real-time RT–PCR, effects of the agent on target gene/*GAPDH* expression were shown as relative values of the vehicle control. In positivity analysis of staining assays and protein expression measurements of WB, effects of the agent were tested using replicates from the same donors. One-way repeated measures analysis of variance (ANOVA) with the Tukey–Kramer post-hoc test was thus used. Normal distributions were evaluated by using the Shapiro–Wilk test as well as the shape of the histogram and boxplot, similarity of mean and median values, and symmetry of the 25th and 75th percentiles.

Consequently, only *ACAN*/*GAPDH* mRNA expression ratios in real-time RT–PCR were not normally distributed. In this analysis, non-parametric Kruskal–Wallis test with the Steel–Dwass post-hoc test was applied.

Data are expressed as the mean ± 95% confidence interval (CI). Statistical analysis was performed using IBM SPSS Statistics 23.0 (IBM, Armonk, NY) or R (https://www.r-project.org/).

Results

Pharmacological mTORC1 inhibition activates Akt and autophagy in human disc NP cells

First, we validated human disc NP cells isolated from surgical specimens, which all showed positive expression of disc NP notochord-phenotypic brachyury and CD24[32]. Furthermore, all cell samples had constant mTOR, p70/S6K, and Akt expression [Fig. 3(A)].

Next, to identify drug toxicity, dose-dependent cell viability was analyzed based on CCK-8. Cell viability significantly decreased by temsirolimus (versus control, 95% CI −0.329 to −0.006) and

Fig. 3. Pharmacological mTORC1 inhibition activates Akt and autophagy in human disc NP cells. (A) WB for disc NP-phenotypic brachyury and CD24 and mTOR signaling-related mTOR, p70/S6K, and Akt in total protein extracts from human disc NP cells of patients who underwent lumbar spine surgery for degenerative disease after 240-h culture in DMEM with 10% FBS. Actin was used as a loading control. Immunoblots show samples randomly selected ($n = 6$). (B) Cell viability of human disc NP cells using CCK-8 after 24-h treatment of 0–50-μM mTORC1-inhibiting rapamycin, temsirolimus, everolimus, or curcumin in DMEM with 10% FBS. Changes in CCK-8 dehydrogenase activity of drug treatment relative to the vehicle control are shown. Data are the mean ± 95% CI. One-way repeated measures ANOVA with the Tukey–Kramer post-hoc test was used ($n = 6$). (C) WB for mTOR signaling-related mTOR, phosphorylated mTOR (p-mTOR), p70/S6K, phosphorylated p70/S6K (p-p70/S6K), Akt, and phosphorylated Akt (p-Akt), autophagy-related LC3 and p62/SQSTM1, and actin in total protein extracts from human disc NP cells after 24-h treatment of 100-nM mTORC1-inhibiting rapamycin, temsirolimus, everolimus, curcumin, or vehicle control in DMEM with 10% FBS. WB for LC3 and actin in human disc NP-cell total protein extracts in 10% FBS-supplemented DMEM with 15-μM chloroquine was also performed to assess LC3 turnover. Immunoblots shown are representative of experiments with similar results ($n = 6$).

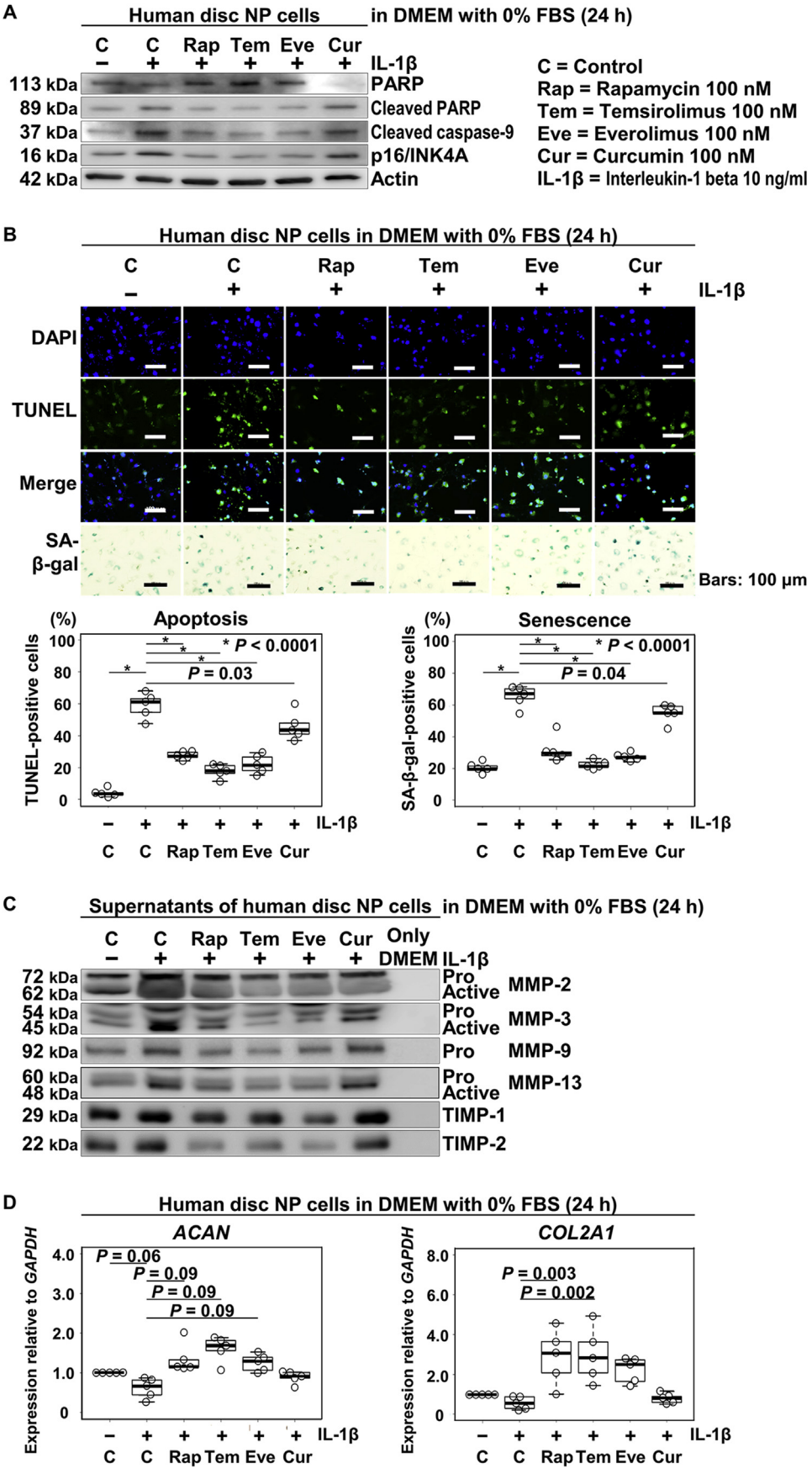
A
Human disc NP cells in DMEM with 0% FBS (24 h)
C C Rap Tem Eve Cur
– + + + + + IL-1β
113 kDa PARP
89 kDa Cleaved PARP
37 kDa Cleaved caspase-9
16 kDa p16/INK4A
42 kDa Actin
C = Control
Rap = Rapamycin 100 nM
Tem = Temsirolimus 100 nM
Eve = Everolimus 100 nM
Cur = Curcumin 100 nM
IL-1β = Interleukin-1 beta 10 ng/ml
B
Human disc NP cells in DMEM with 0% FBS (24 h)
C C Rap Tem Eve Cur
– + + + + + IL-1β
DAPI
TUNEL
Merge
SA-β-gal
Bars: 100 μm
Apoptosis
(%)
TUNEL-positive cells
* P < 0.0001
P = 0.03
Senescence
SA-β-gal-positive cells
P = 0.04
C
Supernatants of human disc NP cells in DMEM with 0% FBS (24 h)
C C Rap Tem Eve Cur Only DMEM IL-1β
72 kDa 62 kDa Pro Active MMP-2
54 kDa 45 kDa Pro Active MMP-3
92 kDa Pro MMP-9
60 kDa 48 kDa Pro Active MMP-13
29 kDa TIMP-1
22 kDa TIMP-2
D
Human disc NP cells in DMEM with 0% FBS (24 h)
ACAN
Expression relative to GAPDH
P = 0.06
P = 0.09
P = 0.09
P = 0.09
COL2A1
P = 0.003
P = 0.002

everolimus (versus control, 95% CI −0.359 to −0.137) at ≥1 μM. To directly compare effectiveness of mTORC1 inhibitors, analysis at the same dose of 100 nM was selected as an effective but non-toxic concentration [Fig. 3(B)].

Then, we assessed mTOR signaling. WB demonstrated that rapamycin, temsirolimus, and everolimus successfully decreased mTOR and down-stream p70/S6K phosphorylation but increased up-stream Akt phosphorylation, although curcumin did not affect these phosphorylation [Fig. 3(C) and Supplemental Table 2]. This Akt activation is through the negative feedback loop from p70/S6K to the class I PI3K[42]. The PI3K is responsible for various cellular functions related to the competence to activate Akt[20].

We further assessed autophagy. WB displayed that rapamycin, temsirolimus, and everolimus increased LC3-II and decreased p62/SQSTM1 [Fig. 3(C) and Supplemental Table 2]. The phosphatidylethanolamine-conjugated form of LC3, LC3-II (unlike its cytosolic form, LC3-I), is the only protein marker reliably associated with completed autophagosomes[33]. The p62/SQSTM1 and p62/SQSTM1-bound polyubiquitinated proteins become incorporated into completed autophagosomes and degraded in autolysosomes, thus serving as an autophagy substrate[33]. Hence, the observed findings are consistent with enhanced autophagy. To make sure increased autophagic flux, LC3 turnover assay using a lysosomotropic compound, chloroquine, was conducted. Chloroquine is known to induce the accumulation of autophagosomes with LC3-II by blocking lysosomal acidification[33]. Chloroquine administration presented increased LC3-II expression under all mTORC1-inhibiting conditions, indicating successful inhibition of LC3-II degradation. Then, the degree of autophagic LC3-II accumulation was most prominent in temsirolimus treatment [Fig. 3(C) and Supplemental Table 2].

Pharmacological mTORC1 inhibition protects against apoptosis, senescence, and matrix catabolism in human disc NP cells

Next, we assessed cell death, aging, and matrix metabolism. WB showed that pro-inflammatory IL-1β stimulation increased PARP and caspase-9 cleavage, indicating apoptosis induction, and p16/INK4A expression, indicating senescence induction. Then, all mTORC1 inhibitors suppressed IL-1β-induced apoptotic and senescent changes. This trend was distinct in rapamycin, temsirolimus, and everolimus [Fig. 4(A) and Supplemental Table 2].

These anti-apoptotic and anti-senescent effects of mTORC1 inhibitors were further confirmed by TUNEL and SA-β-gal staining assays, respectively. The percentage of TUNEL-positive cells increased by IL-1β (versus control, 95% CI 0.429 to 0.666). This change was suppressed by mTORC1 inhibitors (IL-1β vs IL-1β&rapamycin, 95% CI −0.431 to −0.194; IL-1β&temsirolimus, 95% CI −0.529 to −0.292; IL-1β&everolimus, 95% CI −0.477 to −0.241; IL-1β&curcumin, 95% CI −0.248 to −0.011). The SA-β-gal-positive cell percentage increased by IL-1β (versus control, 95% CI 0.345 to 0.552), which was also suppressed by mTORC1 inhibitors (IL-1β vs IL-1β&rapamycin, 95% CI −0.437 to −0.230; IL-1β&temsirolimus, 95% CI −0.534 to −0.327; IL-1β&everolimus, 95% CI −0.485 to −0.278; IL-1β&curcumin, 95% CI −0.210 to −0.003) [Fig. 4(B)].

In culture supernatants, IL-1β induced the shift of matrix metabolism toward catabolism showing drastically increased catabolic MMP-2, MMP-3, MMP-9 and MMP-13 and anti-catabolic TIMP-1 and TIMP-2. These release was markedly reduced by rapamycin, temsirolimus, and everolimus [Fig. 4(C) and Supplemental Table 2].

Real-time RT–PCR further demonstrated the trend toward IL-1β-induced down-regulation of anabolic *ACAN* (versus control, $P = 0.06$) and *COL2A1* genes (versus control, 95% CI −2.101 to 1.220). Then, the first generation mTOR inhibitors showed the tendency toward up-regulation of *ACAN* (IL-1β vs IL-1β&rapamycin, $P = 0.09$; IL-1β&temsirolimus, $P = 0.09$; IL-1β&everolimus, $P = 0.09$) and *COL2A1* mRNA expression (IL-1β vs IL-1β&rapamycin, 95% CI 0.652 to 3.974; IL-1β&temsirolimus, 95% CI 0.764 to 4.086; IL-1β&everolimus, 95% CI −0.010 to 3.312) [Fig. 4(D)]. All the tested mTORC1 inhibitors induce anti-apoptosis, anti-senescence, and anti-matrix catabolism—notably, temsirolimus.

Pharmacological dual mTOR inhibition does not protect against apoptosis, senescence, and matrix catabolism in human disc NP cells

We further tested the second generation mTOR inhibitors. We selected INK-128 to block mTORC1 and mTORC2 and NVP-BEZ235 to block PI3K and both mTOR complexes, which are under clinical trials for advanced solid tumors[27]. Reduced cell viability was observed at ≥1 μM of INK-128 (versus control, 95% CI −0.523 to −0.182) and ≥100 nM of NVP-BEZ235 (versus control, 95% CI −0.498 to −0.223). Hence, 100 nM was selected to compare effects at the same dose as the tested mTORC1 inhibitors [Fig. 5(A)].

WB showed that INK-128 and NVP-BEZ235 both decreased mTOR, p70/S6K, and then Akt phosphorylation, indicating successful extensive mTOR inhibition. However, both treatments displayed neither marked increases in LC3-II nor decreases in p62/SQSTM1. The LC3 turnover assay also revealed no obvious increases in LC3-II. Despite distinct mTORC1 inhibition, the tested dual mTOR inhibitors did not induce autophagy [Fig. 5(B) and Supplemental Table 2].

Unlike mTORC1 inhibitors, WB demonstrated that INK-128 and NVP-BEZ235 did not suppress IL-1β-induced increases in apoptotic cleaved PARP and cleaved caspase-9 and senescent p16/INK4A. Actually, both these agents accelerated these apoptotic and senescent changes [Fig. 5(C) and Supplemental Table 2].

In culture supernatants, WB displayed that INK-128 and NVP-BEZ235 did not reduce IL-1β-induced release and activation of catabolic MMP-2, MMP-3, MMP-9, and MMP-13. Anti-catabolic TIMP-1 and TIMP-2 production by IL-1β was also not affected substantially [Fig. 5(D) and Supplemental Table 2]. The second generation mTOR inhibitors do not rescue human disc cells against inflammation.

Pro-autophagic, anti-apoptotic, anti-senescent, and anti-catabolic effects of mTORC1 inhibition depend on Akt activation in human disc NP cells

Our findings raised the hypothesis that beneficial effects of mTORC1 inhibitors would depend on Akt activation. Therefore, we

Fig. 4. Pharmacological mTORC1 inhibition protects against apoptosis, senescence, and matrix catabolism in human disc NP cells. (A) WB for apoptotic PARP, cleaved PARP, and cleaved caspase-9 and senescent p16/INK4A in total protein extracts from human disc NP cells after 24-h treatment of 100-nM mTORC1-inhibiting rapamycin, temsirolimus, everolimus, curcumin, or vehicle control in serum-free DMEM with or without 10-ng/ml IL-1β. Actin was used as a loading control. (B) Immunofluorescence for apoptotic TUNEL (green), nuclear DAPI (blue), and merged signals and cytochemical SA-β-gal staining for senescence detection in human disc NP cells after the same treatment. Changes in the percentage of TUNEL-positive cells in DAPI-positive cells and of SA-β-gal-positive cells in total cells are shown. The number of cells was counted in six random low-power fields (×100). Data are the mean ± 95% CI. One-way repeated measures ANOVA with the Tukey–Kramer post-hoc test was used ($n = 6$). (C) WB for catabolic MMP-2, MMP-3, MMP-9, and MMP-13 and anti-catabolic TIMP-1 and TIMP-2 in supernatant protein extracts from human disc NP cells after the same treatment. (D) Real-time RT–PCR for anabolic *ACAN* and *COL2A1* in total RNA extracts from human disc NP cells after the same treatment. *GAPDH* was used as an endogenous control. Changes in *ACAN*/*GAPDH* and *COL2A1*/*GAPDH* mRNA expression of drug and IL-1β treatment relative to the vehicle control are shown. Data are the mean ± 95% CI. Based on the normality of data distributions, one-way repeated measures ANOVA with the Tukey–Kramer post-hoc test was used for *COL2A1* while the Kruskal–Wallis test with the Steel–Dwass post-hoc test was used for *ACAN* ($n = 6$). In (A), (B), and (C), immunoblots and images shown are representative of experiments with similar results ($n = 6$).

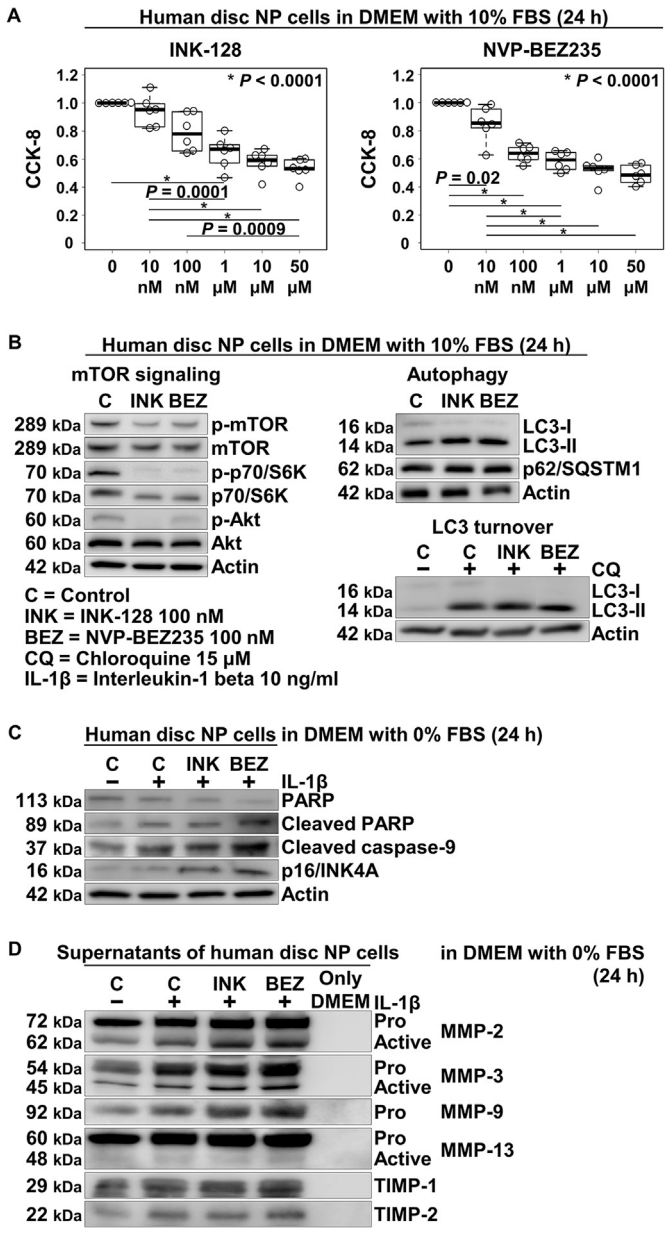

Fig. 5. Pharmacological dual mTOR inhibition does not protect against apoptosis, senescence, and matrix catabolism in human disc NP cells. (A) Cell viability of human disc NP cells using CCK-8 after 24-h treatment of 0–50-μM mTORC1-inhibiting and mTORC2-inhibiting INK-128 or PI3K-inhibiting and mTOR-inhibiting NVP-BEZ235 in DMEM with 10% FBS. Changes in CCK-8 dehydrogenase activity of drug treatment relative to the vehicle control are shown. Data are the mean ± 95% CI. One-way repeated measures ANOVA with the Tukey–Kramer post-hoc test was used ($n = 6$). (B) WB for mTOR signaling-related mTOR, phosphorylated mTOR (p-mTOR), p70/S6K, phosphorylated p70/S6K (p-p70/S6K), Akt, and phosphorylated Akt (p-Akt) and autophagy-related LC3 and p62/SQSTM1 in total protein extracts from human disc NP cells after 24-h treatment of 100-nM INK-128, NVP-BEZ235, or vehicle control in DMEM with 10% FBS. Actin was used as a loading control. WB for LC3 and actin in human disc NP-cell total protein extracts in 10% FBS-supplemented DMEM with 15-μM chloroquine was also performed to assess LC3 turnover. (C) WB for apoptotic PARP, cleaved PARP, and cleaved caspase-9, senescent p16/INK4A, and actin in total protein extracts from human disc NP cells after 24-h treatment of 100-nM INK-128, NVP-BEZ235, or vehicle control in serum-free DMEM with or without 10-ng/ml IL-1β. (D) WB for catabolic MMP-2, MMP-3, MMP-9, and MMP-13 and anti-catabolic TIMP-1 and TIMP-2 in supernatant protein extracts from human disc NP cells after the same treatment. In (B), (C), and (D), immunoblots shown are representative of experiments with similar results ($n = 6$).

tested an allosteric Akt inhibitor, MK-2206, which is also under clinical trials for renal cell carcinoma[29]. We analyzed the combined administration of temsirolimus and MK-2206 as well as the independent administration of MK-2206. The CCK-8 assay demonstrated dose-dependent cell toxicity by MK-2206 at ≥5 μM (versus control, 95% CI −0.794 to −0.268). We selected 5 μM as a tested concentration of MK-2206 based on prior reports [Fig. 6(A)][43].

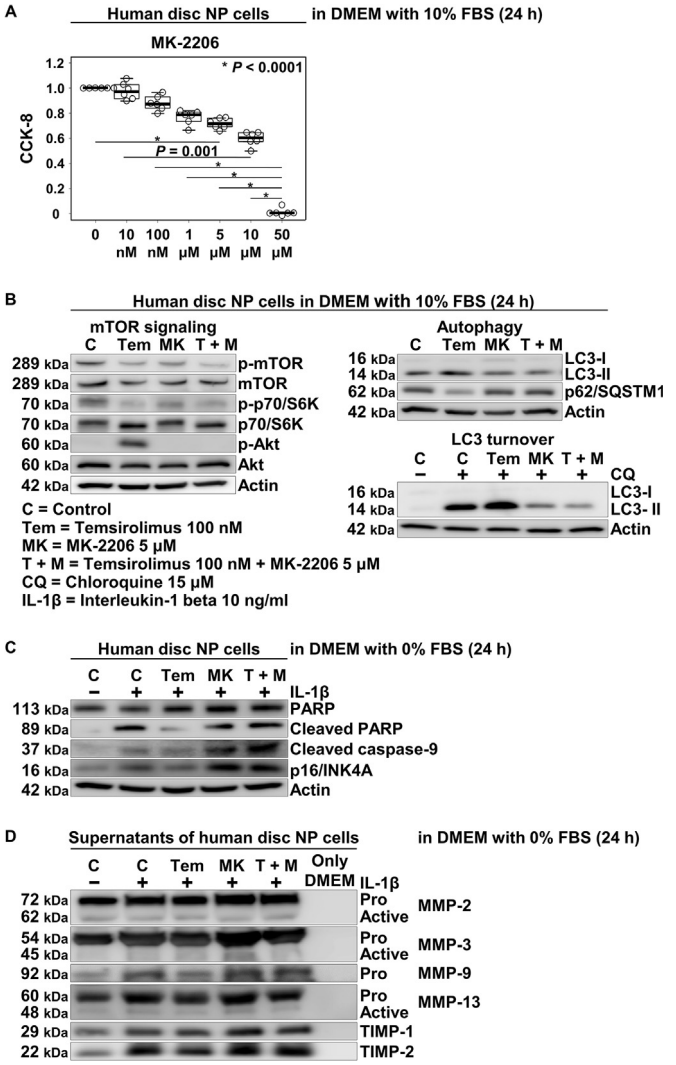

Fig. 6. Pro-autophagic, anti-apoptotic, anti-senescent, and anti-catabolic effects of mTORC1 inhibition depend on Akt activation in human disc NP cells. (A) Cell viability of human disc NP cells using CCK-8 after 24-h treatment of 0–50-μM Akt-inhibiting MK-2206 in DMEM with 10% FBS. Changes in CCK-8 dehydrogenase activity of drug treatment relative to the vehicle control are shown. Data are the mean ± 95% CI. One-way repeated measures ANOVA with the Tukey–Kramer post-hoc test was used ($n = 6$). (B) WB for mTOR signaling-related mTOR, phosphorylated mTOR (p-mTOR), p70/S6K, phosphorylated p70/S6K (p-p70/S6K), Akt, and phosphorylated Akt (p-Akt) and autophagy-related LC3 and p62/SQSTM1 in total protein extracts from human disc NP cells after 24-h treatment of 100-nM mTORC1-inhibiting temsirolimus, 5-μM MK-2206, combined 100-nM temsirolimus and 5-μM MK-2206, or vehicle control in DMEM with 10% FBS. Actin was used as a loading control. WB for LC3 and actin in human disc NP-cell total protein extracts in 10% FBS-supplemented DMEM with 15-μM chloroquine was also performed to assess LC3 turnover. (C) WB for apoptotic PARP, cleaved PARP, and cleaved caspase-9, senescent p16/INK4A, and actin in total protein extracts from human disc NP cells after 24-h treatment of 100-nM temsirolimus, 5-μM MK-2206, combined 100-nM temsirolimus and 5-μM MK-2206, or vehicle control in serum-free DMEM with or without 10-ng/ml IL-1β. (D) WB for catabolic MMP-2, MMP-3, MMP-9, and MMP-13 and anti-catabolic TIMP-1 and TIMP-2 in supernatant protein extracts from human disc NP cells after the same treatment. In (B), (C), and (D), immunoblots shown are representative of experiments with similar results ($n = 6$).

WB showed that MK-2206 with or without temsirolimus decreased mTOR, p70/S6K, and Akt phosphorylation, indicating successful Akt inhibition. However, MK-2206 presented unchanged LC3-II and p62/SQSTM1 expression, indicating autophagy non-activation. The LC3 turnover assay further exhibited decreased autophagic flux [Fig. 6(B) and Supplemental Table 2].

Under IL-1β stimulation, increases in apoptotic and senescent markers were suppressed by temsirolimus but further enhanced by MK-2206, clearly indicating up-stream regulation of cell death and aging by Akt [Fig. 6(C) and Supplemental Table 2].

Similarly, catabolic MMP and anti-catabolic TIMP release by IL-1β was suppressed by temsirolimus but further exaggerated by MK-2206, suggesting the maintenance of matrix homeostasis by Akt [Fig. 6(D) and Supplemental Table 2]. Based on anti-autophagic, pro-apoptotic, pro-senescent, and pro-catabolic findings of Akt inhibition by MK-2206, protective effects of temsirolimus against inflammation primarily depend on Akt activation in human disc cells.

mTOR signaling has relevance to degeneration grades in human disc NP tissues

Additionally, we examined *in vivo* involvement of mTOR signaling in human disc NP surgical specimens. WB showed relatively maintained expression of disc NP-phenotypic brachyury and CD24, which subsequently decreased in discs with advanced ages and degeneration grades. Expression of mTOR, p70/S6K, and Akt was detectable in all discs with 19 to 81 in ages and 2 to 5 in degeneration grades. Phosphorylation of mTOR, p70/S6K, and Akt was also detectable. Furthermore, mTOR, p70/S6K, and Akt expression and phosphorylation were all marked in Pfirrmann grade-3 discs, although it did not provide conclusive evidence from viewpoints of the sample size and variation in *in vivo* tissues [Fig. 7].

Discussion

This is the first mechanistic study by using clinically available drugs to demonstrate cascade-dependent, differential roles of mTOR signaling in human intervertebral disc cells. We tested mTORC1 inhibitors—rapamycin, temsirolimus, everolimus, and curcumin, revealing decreased mTOR and p70/S6K but increased Akt phosphorylation. All these agents provided consistent pro-autophagic, anti-apoptotic, anti-senescent, and anti-catabolic effects. Autophagy is negatively regulated by mTORC1[20]. Apoptosis can be suppressed by Akt activation through the negative feedback loop from p70/S6K[42]. The Akt promotes cell survival directly by blocking pro-apoptotic proteins including the Bcl-2-associated death promoter protein and through effects on transcription factors such as forkhead box O and p53[21]. Senescence would also be affected by mTORC1 that controls cell cycle and proliferation positively through p70/S6K and negatively through eukaryotic translation initiation factor 4E-binding protein 1 (4E-BP1)[20]. Dietary restriction-induced lifespan extension requires 4E-BP1[44]. Lifespan extension is also accomplished by p70/S6K deletion[45]. Mice with hypomorphic mTOR (approximately 25% of wild-type levels) have shown increased lifespan and reduced aging tissue biomarkers, e.g., p16/INK4A[46]. Furthermore, mice with articular cartilage-specific mTOR deletion have shown to be protective against destabilized medial meniscus-induced osteoarthritis based on enhanced autophagy, decreased apoptosis, and then increased catabolic MMP-13 expression[47]. In matrix metabolism, we previously reported a possible regulation of MMP expression and activation by mTORC1 and p70/S6K-mediated translation[23]. In this study, the optimal effectiveness of temsirolimus is noteworthy. This potentially results from an improved water solubility that enables intravenous administration while others are approved only for oral administration[28]. Meanwhile, curcumin was not toxic but less effective. A poor aqueous solubility, low bioavailability, and intense staining color of curcumin have been reported as problems[48]. Therefore, we selected temsirolimus as a candidate of the optimal mTORC1 inhibitor for human disc disease [Fig. 8]. When clinical applications of temsirolimus are considered, adverse immunosuppression would recommend its local intra-discal injection rather than systemic administration.

The second generation mTOR inhibitors that can block multiple mTOR-signaling components have been developed for cancer treatment[27]. These agents have been proven to be more powerful than mTORC1 inhibitors in reduced protein synthesis and attenuated cell-cycle progression[27]. In this study, the tested dual mTOR inhibitors—INK-128 and BEZ-NVP235—both decreased mTOR, p70/S6K, and Akt phosphorylation. Then, INK-128 and BEZ-NVP235 accelerated disc cell apoptosis, which can be explained by mTORC2

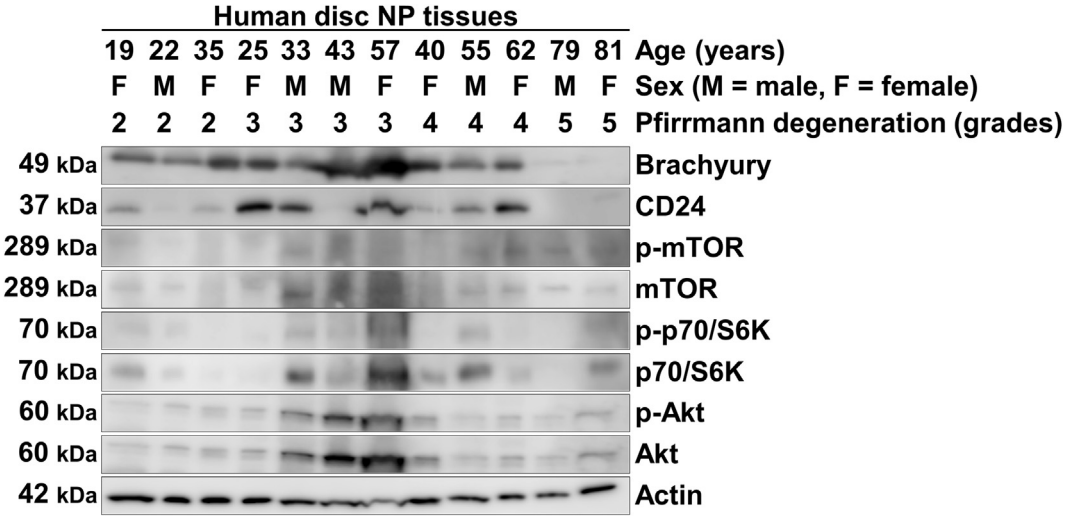

Fig. 7. mTOR signaling has relevance to degeneration grades in human disc NP tissues. WB for disc NP-phenotypic brachyury and CD24 and mTOR signaling-related mTOR, phosphorylated mTOR (p-mTOR), p70/S6K, phosphorylated p70/S6K (p-p70/S6K), Akt, and phosphorylated Akt (p-Akt) in total protein extracts from human disc NP tissues of patients who underwent lumbar spine surgery for degenerative disease. Actin was used as a loading control. Immunoblots show samples randomly selected ($n = 12$).

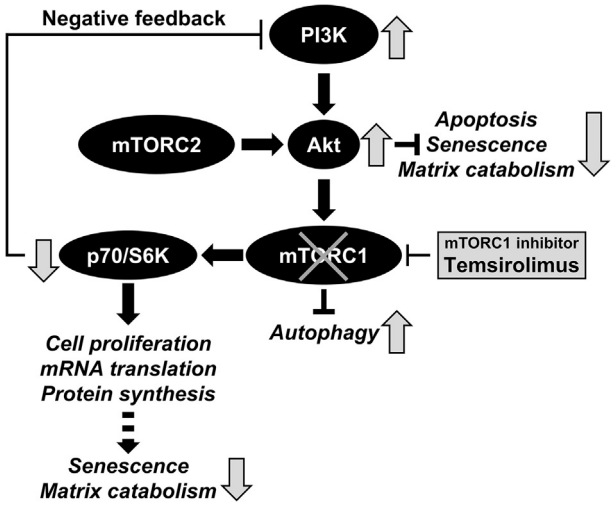

Fig. 8. Schematic illustration of effects of mTORC1 inhibition by temsirolimus on human disc NP cells. The mTOR is a serine/threonine kinase that integrates nutrients to execute cell growth and division. The mTOR exists in two complexes of mTORC1 and mTORC2. Down-stream effectors of mTORC1 including p70/S6K regulate cell proliferation, mRNA translation, and protein synthesis. Autophagy is under the tight negative regulation of mTORC1. The mTORC1 is regulated by the up-stream class I PI3K followed by Akt, an essential pro-survival mediator by suppressing apoptosis. Senescence and matrix catabolism are also affected by mTOR signaling. In human disc NP cells, mTORC1 inhibition by temsirolimus decreased p70/S6K phosphorylation but increased Akt phosphorylation through the negative feedback loop for the class I PI3K. Furthermore, mTORC1 inhibition by temsirolimus suppressed apoptosis, senescence, and matrix catabolism as well as enhanced autophagy, depending on Akt activation primarily.

inhibition-mediated Akt suppression[27]. Furthermore, these agents stimulated disc cellular senescence and matrix catabolism. The Akt increases cell proliferation through not only mTORC1 induction (p70/S6K induction and 4E-BP1 inhibition) but also other pathways including inhibition of negative cell-cycle regulators p27/KIP1 and p21/CIP1[21]. The mitogen-activated protein kinase signaling, a major cascade of catabolic MMP production and activation[7], has Akt-dependent inactivation[21]. Our findings indicate that dual mTOR inhibitors are not helpful for human disc cells due to Akt suppression.

To determine the direct evidence of Akt roles in human disc cells, we tested an allosteric Akt inhibitor—MK-2206. In the independent and also combined use with mTORC1-inhibiting temsirolimus, MK-2206 showed a marked inhibition of Akt phosphorylation, subsequently resulting in decreased mTOR and p70/S6K phosphorylation. Furthermore, Akt inhibition by MK-2206 clearly diminished anti-apoptotic, anti-senescent, and anti-catabolic effects of temsirolimus. In mice, Akt1 controls endochondral ossification in skeletal growth and osteophyte formation in osteoarthritis[49]. Thus, the present study disclose that Akt is the key regulator of mTOR signaling in human disc cells.

Interestingly, despite the negative regulation of autophagy by mTORC1 followed by Akt[20], dual mTOR inhibitors and MK-2206 with extensive suppression of PI3K/Akt/mTOR signaling did not activate autophagy in human disc cells. Similar responses were observed in human lymphoblasts, in which accelerated autophagy at early time points but switched autophagy to apoptosis were observed by MK-2206 augmentation[50]. Anti-apoptotic and anti-senescent effects of autophagy are well reported[18,23,25,33]. Further investigations for autophagy regulation through the Akt-signaling network in disc cells are required.

Our disc-tissue WB previously found age-dependent decreases in Akt expression and phosphorylation[23]. In this study, we further reported increases in mTOR, p70/S6K, and Akt expression and phosphorylation of grade-3 discs. Despite the increased interest of mTOR signaling[20], its actual involvement in disc degeneration is largely unknown. The observed mTOR-signaling molecule expression and phosphorylation with aging and degeneration grades are potentially supportive to disclose the involvement in disc health. However, due to the variation in *in vivo* expression and phosphorylation levels of intracellular signaling molecules, future examinations with larger sample sizes are required to obtain conclusive evidence.

This study lacks *in vivo* drug treatment data. To clarify impacts of biological mTOR-modulating therapies, we are conducting animal model studies of disc degeneration[10–12,15,39]. Another limitation is the monolayer cell culture. Three-dimensional culture systems are favorable to simulate the physiological environment of the disc NP; however, it was difficult to analyze detailed molecular signaling using alginate gel beads. An additional limitation is limited consideration of variations in age, sex, and disc degeneration grade, although the current *in vitro* findings were consistent regardless these parameters. These are subjects to be studied in the future.

In conclusion, mTORC1 inhibitors but not dual mTOR inhibitors protect against inflammation-induced apoptosis, senescence, and matrix catabolism in human disc cells. Beneficial effects of mTORC1 inhibitors—notably temsirolimus with an improved water solubility—depend on the induction of Akt as well as autophagy, providing insight into biological therapy.

Authors' contributions

All authors have made substantial contributions to (1) the conception and design of the study, or acquisition of data, or analysis and interpretation of data; (2) drafting the article or revising it critically for important intellectual content; and (3) final approval of the version to be submitted. The specific contributions of the authors are as follows:

(1) Conception and design of the study: YKakiuchi, TY
(2) Analysis and interpretation of the data: YKakiuchi, TY, KK, TT, MI, YT, YKanda, SM, RK, KN
(3) Drafting of the article: YKakiuchi, TY
(4) Critical revision of the article for important intellectual content: KK, TT, MI, YT, YKanda, SM, RK, KN
(5) Final approval of the article: YKakiuchi, TY, KK, TT, MI, YT, YKanda, SM, RK, KN
(6) Statistical expertise: YKakiuchi, TY
(7) Collection and assembly of data: YKakiuchi, TY.

Competing interests

The authors have no competing interests to declare.

Role of the funding source

This work was supported by JSPS KAKENHI Grant Numbers JP26893151, JP15H03033, JP15K10406, and JP16K20051 and a Grant of Japan Orthopaedics and Traumatology Research Foundation, Inc. Number 312. The study sponsors had no involvement in this study.

Acknowledgements

The authors thank Dr. Daisuke Sugiyama (Department of Preventive Medicine and Public Health, Keio University School of Medicine, Tokyo, Japan) for his statistical advice and Mses. Kyoko Tanaka, Maya Yasuda, and Minako Nagata for their technical assistance.

Supplementary data

Supplementary data to this article can be found online at https://doi.org/10.1016/j.joca.2019.01.009.

References

1. Andersson GB. Epidemiological features of chronic low-back pain. Lancet 1999;354:581–5.
2. Katz JN. Lumbar disc disorders and low-back pain: socioeconomic factors and consequences. J Bone Jt Surg Am 2006;88(Suppl 2):21–4.
3. Livshits G, Popham M, Malkin I, Sambrook PN, Macgregor AJ, Spector T, *et al*. Lumbar disc degeneration and genetic factors are the main risk factors for low back pain in women: the UK Twin Spine Study. Ann Rheum Dis 2011;70:1740–5.
4. Urban JP, Roberts S. Degeneration of the intervertebral disc. Arthritis Res Ther 2003;5:120–30.
5. Urban JP, Smith S, Fairbank JC. Nutrition of the intervertebral disc. Spine (Phila Pa 1976) 2004;29:2700–9.
6. Antoniou J, Steffen T, Nelson F, Winterbottom N, Hollander AP, Poole RA, *et al*. The human lumbar intervertebral disc: evidence for changes in the biosynthesis and denaturation of the extracellular matrix with growth, maturation, ageing, and degeneration. J Clin Invest 1996;98:996–1003.
7. Vo NV, Hartman RA, Yurube T, Jacobs LJ, Sowa GA, Kang JD. Expression and regulation of metalloproteinases and their inhibitors in intervertebral disc aging and degeneration. Spine J 2013;13:331–41.
8. Kanemoto M, Hukuda S, Komiya Y, Katsuura A, Nishioka J. Immunohistochemical study of matrix metalloproteinase-3 and tissue inhibitor of metalloproteinase-1 human intervertebral discs. Spine (Phila Pa 1976) 1996;21:1–8.
9. Roberts S, Caterson B, Menage J, Evans EH, Jaffray DC, Eisenstein SM. Matrix metalloproteinases and aggrecanase: their role in disorders of the human intervertebral disc. Spine (Phila Pa 1976) 2000;25:3005–13.
10. Yurube T, Nishida K, Suzuki T, Kaneyama S, Zhang Z, Kakutani K, *et al*. Matrix metalloproteinase (MMP)-3 gene upregulation in a rat tail compression loading-induced disc degeneration model. J Orthop Res 2010;28:1026–32.
11. Yurube T, Takada T, Suzuki T, Kakutani K, Maeno K, Doita M, *et al*. Rat tail static compression model mimics extracellular matrix metabolic imbalances of matrix metalloproteinases, aggrecanases, and tissue inhibitors of metalloproteinases in intervertebral disc degeneration. Arthritis Res Ther 2012;14:R51.
12. Hirata H, Yurube T, Kakutani K, Maeno K, Takada T, Yamamoto J, *et al*. A rat tail temporary static compression model reproduces different stages of intervertebral disc degeneration with decreased notochordal cell phenotype. J Orthop Res 2014;32:455–63.
13. Fuchs Y, Steller H. Programmed cell death in animal development and disease. Cell 2011;147:742–58.
14. Gruber HE, Hanley Jr EN. Analysis of aging and degeneration of the human intervertebral disc. Comparison of surgical specimens with normal controls. Spine (Phila Pa 1976) 1998;23:751–7.
15. Yurube T, Hirata H, Kakutani K, Maeno K, Takada T, Zhang Z, *et al*. Notochordal cell disappearance and modes of apoptotic cell death in a rat tail static compression-induced disc degeneration model. Arthritis Res Ther 2014;16:R31.
16. Lombard DB, Chua KF, Mostoslavsky R, Franco S, Gostissa M, Alt FW. DNA repair, genome stability, and aging. Cell 2005;120:497–512.
17. Le Maitre CL, Freemont AJ, Hoyland JA. Accelerated cellular senescence in degenerate intervertebral discs: a possible role in the pathogenesis of intervertebral disc degeneration. Arthritis Res Ther 2007;9:R45.
18. Levine B, Kroemer G. Autophagy in the pathogenesis of disease. Cell 2008;132:27–42.
19. Gruber HE, Hoelscher GL, Ingram JA, Bethea S, Hanley Jr EN. Autophagy in the degenerating human intervertebral disc: in vivo molecular and morphological evidence, and induction of autophagy in cultured annulus cells exposed to proinflammatory cytokines-implications for disc degeneration. Spine (Phila Pa 1976) 2015;40:773–82.
20. Zoncu R, Efeyan A, Sabatini DM. mTOR: from growth signal integration to cancer, diabetes and ageing. Nat Rev Mol Cell Biol 2011;12:21–35.
21. Manning BD, Cantley LC. AKT/PKB signaling: navigating downstream. Cell 2007;129:1261–74.
22. Murakami M, Ichisaka T, Maeda M, Oshiro N, Hara K, Edenhofer F, *et al*. mTOR is essential for growth and proliferation in early mouse embryos and embryonic stem cells. Mol Cell Biol 2004;24:6710–8.
23. Ito M, Yurube T, Kakutani K, Maeno K, Takada T, Terashima Y, *et al*. Selective interference of mTORC1/RAPTOR protects against human disc cellular apoptosis, senescence, and extracellular matrix catabolism with Akt and autophagy induction. Osteoarthritis Cartilage 2017;25:2134–46.
24. Harrison DE, Strong R, Sharp ZD, Nelson JF, Astle CM, Flurkey K, *et al*. Rapamycin fed late in life extends lifespan in genetically heterogeneous mice. Nature 2009;460:392–5.
25. Sasaki H, Takayama K, Matsushita T, Ishida K, Kubo S, Matsumoto T, *et al*. Autophagy modulates osteoarthritis-related gene expression in human chondrocytes. Arthritis Rheum 2012;64:1920–8.
26. Cravedi P, Ruggenenti P, Remuzzi G. Sirolimus to replace calcineurin inhibitors? Too early yet. Lancet 2009;373:1235–6.
27. Zaytseva YY, Valentino JD, Gulhati P, Evers BM. mTOR inhibitors in cancer therapy. Cancer Lett 2012;319:1–7.
28. Zhou H, Luo Y, Huang S. Updates of mTOR inhibitors. Anti Cancer Agents Med Chem 2010;10:571–81.
29. Jonasch E, Hasanov E, Corn PG, Moss T, Shaw KR, Stovall S, *et al*. A randomized phase 2 study of MK-2206 versus everolimus in refractory renal cell carcinoma. Ann Oncol 2017;28:804–8.
30. Pfirrmann CW, Metzdorf A, Zanetti M, Hodler J, Boos N. Magnetic resonance classification of lumbar intervertebral disc degeneration. Spine (Phila Pa 1976) 2001;26:1873–8.
31. Risbud MV, Shapiro IM. Role of cytokines in intervertebral disc degeneration: pain and disc content. Nat Rev Rheumatol 2014;10:44–56.
32. Risbud MV, Schoepflin ZR, Mwale F, Kandel RA, Grad S, Iatridis JC, *et al*. Defining the phenotype of young healthy nucleus pulposus cells: recommendations of the Spine Research Interest Group at the 2014 annual ORS meeting. J Orthop Res 2015;33:283–93.
33. Klionsky DJ, Abdelmohsen K, Abe A, Abedin MJ, Abeliovich H, Acevedo Arozena A, *et al*. Guidelines for the use and interpretation of assays for monitoring autophagy (3rd edition). Autophagy 2016;12:1–222.
34. Yu SW, Andrabi SA, Wang H, Kim NS, Poirier GG, Dawson TM, *et al*. Apoptosis-inducing factor mediates poly(ADP-ribose) (PAR) polymer-induced cell death. Proc Natl Acad Sci U S A 2006;103:18314–9.
35. Li P, Nijhawan D, Budihardjo I, Srinivasula SM, Ahmad M, Alnemri ES, *et al*. Cytochrome c and dATP-dependent formation of Apaf-1/caspase-9 complex initiates an apoptotic protease cascade. Cell 1997;91:479–89.

36. Krishnamurthy J, Torrice C, Ramsey MR, Kovalev GI, Al-Regaiey K, Su L, *et al*. Ink4a/Arf expression is a biomarker of aging. J Clin Invest 2004;114:1299–307.
37. Gavrieli Y, Sherman Y, Ben-Sasson SA. Identification of programmed cell death in situ via specific labeling of nuclear DNA fragmentation. J Cell Biol 1992;119:493–501.
38. Dimri GP, Lee X, Basile G, Acosta M, Scott G, Roskelley C, *et al*. A biomarker that identifies senescent human cells in culture and in aging skin in vivo. Proc Natl Acad Sci U S A 1995;92:9363–7.
39. Yurube T, Takada T, Hirata H, Kakutani K, Maeno K, Zhang Z, *et al*. Modified house-keeping gene expression in a rat tail compression loading-induced disc degeneration model. J Orthop Res 2011;29:1284–90.
40. Vo NV, Sowa GA, Kang JD, Seidel C, Studer RK. Prostaglandin E2 and prostaglandin F2alpha differentially modulate matrix metabolism of human nucleus pulposus cells. J Orthop Res 2010;28:1259–66.
41. Livak KJ, Schmittgen TD. Analysis of relative gene expression data using real-time quantitative PCR and the 2(-Delta Delta C(T)) Method. Methods 2001;25:402–8.
42. O'Reilly KE, Rojo F, She QB, Solit D, Mills GB, Smith D, *et al*. mTOR inhibition induces upstream receptor tyrosine kinase signaling and activates Akt. Cancer Res 2006;66:1500–8.
43. Hirai H, Sootome H, Nakatsuru Y, Miyama K, Taguchi S, Tsujioka K, *et al*. MK-2206, an allosteric Akt inhibitor, enhances antitumor efficacy by standard chemotherapeutic agents or molecular targeted drugs in vitro and in vivo. Mol Cancer Ther 2010;9:1956–67.
44. Zid BM, Rogers AN, Katewa SD, Vargas MA, Kolipinski MC, Lu TA, *et al*. 4E-BP extends lifespan upon dietary restriction by enhancing mitochondrial activity in Drosophila. Cell 2009;139:149–60.
45. Selman C, Tullet JM, Wieser D, Irvine E, Lingard SJ, Choudhury AI, *et al*. Ribosomal protein S6 kinase 1 signaling regulates mammalian life span. Science 2009;326:140–4.
46. Wu JJ, Liu J, Chen EB, Wang JJ, Cao L, Narayan N, *et al*. Increased mammalian lifespan and a segmental and tissue-specific slowing of aging after genetic reduction of mTOR expression. Cell Rep 2013;4:913–20.
47. Zhang Y, Vasheghani F, Li YH, Blati M, Simeone K, Fahmi H, *et al*. Cartilage-specific deletion of mTOR upregulates autophagy and protects mice from osteoarthritis. Ann Rheum Dis 2015;74:1432–40.
48. Mendonca LM, Machado Cda S, Teixeira CC, Freitas LA, Bianchi ML, Antunes LM. Comparative study of curcumin and curcumin formulated in a solid dispersion: evaluation of their antigenotoxic effects. Genet Mol Biol 2015;38:490–8.
49. Fukai A, Kawamura N, Saito T, Oshima Y, Ikeda T, Kugimiya F, *et al*. Akt1 in murine chondrocytes controls cartilage calcification during endochondral ossification under physiologic and pathologic conditions. Arthritis Rheum 2010;62:826–36.
50. Cheng Y, Zhang Y, Zhang L, Ren X, Huber-Keener KJ, Liu X, *et al*. MK-2206, a novel allosteric inhibitor of Akt, synergizes with gefitinib against malignant glioma via modulating both autophagy and apoptosis. Mol Cancer Ther 2012;11:154–64.